18. Wang, W. M., Wan, H. H., Rong, T. W., Bao, J. R. and Lin, S. H., Diode characteristics and degradation mechanism of ion implanted polyacetylene films. *Nucl. Instrum. Meth. Phys. Res. B*, 1991, **61**, 466–471.
19. Wang, W. M., Lin, S. H., Bao, J. R., Rong, T. W., Wan, H. H. and Sun, J., The *n*-type doping of polyaniline films by ion implantation. *Nucl. Instrum. Meth. Phys. Res. B*, 1993, **74**, 514–518.
20. Lin, S. H. *et al.*, Electrical properties of chemical-doped and ion-implanted polyacetylene films. *Nucl. Instrum. Meth. Phys. Res. B*, 1991, **59/60**, 1257–1262.
21. Hussain, A. M. P., Kumar, A., Singh, F. and Avasthi, D. K., Effects of 160 MeV Ni^{12+} ion irradiation on HCl doped polyaniline electrode. *J. Phys. D: Appl. Phys.*, 2006, **39**, 750–755.
22. Park, S. K., Lee, S. Y., Lee, C. S., Kim, H. M., Joo, J., Beag, Y. W. and Koh, S. K., High energy (MeV) ion-irradiated π-conjugated polyaniline: transition from insulating state to carbonized conducting state. *J. Appl. Phys.*, 2004, **96**, 1914–1918.
23. Tsukuda, S., Seki, S., Sugimoto, M. and Tagawa, S., Formation of nanowires based on π-conjugated polymers by high-energy ion beam irradiation. *Jpn. J. Appl. Phys.*, 2005, **44**, 5839–5842.
24. Tsukuda, S., Seki, S., Sugimoto, M., Tagawa, S., Idesaki, A., Tanaka, S. and Oshima, A., Fabrication of nanowires using high-energy ion beams. *J. Phys. Chem. B*, 2004, **108**, 3407–3409.
25. Srivastava, M. P., Mohanty, S. R., Annapoorni, S. and Rawat, R. S., Diode like behaviour of an ion irradiated polyaniline film. *Phys. Lett. A*, 1996, **215**, 63–68.
26. Venkatesan, T., High energy ion beam modification of polymer films. *Nucl. Instrum. Meth. Phys. Res. B*, 1984, **7–8**, 461–467.
27. Said, M. A., Balik, C. M. and Carlson, J. D., High-energy ion implantation of polymers: poly(vinylidene fluoride). *J. Polym. Sci. B: Polym. Phys.*, 1988, **26**, 1457–1467.
28. Kumar, R., De, U. and Prasad, R., Physical and chemical response of 70 MeV carbon ion irradiated polyether sulphone polymer. *Nucl. Instrum. Meth. Phys. Res. B*, 2006, **248**, 279–283.
29. Kumar, R., Prasad, R., Vijay, Y. K., Acharya, N. K., Verma, K. C. and De, U., Ion beam modification of CR-39 (DOP) and polyamide nylon-6 polymers. *Nucl. Instrum. Meth. Phys. Res. B*, 2003, **212**, 221–227.
30. Virk, H. S., Chandi, P. S. and Srivastava, A. K., Physical and chemical response of 70 MeV carbon ion irradiated Kapton-H polymer. *Bull. Mater. Sci.*, 2001, **24**, 529–534.
31. Virk, H. S., Chadi, P. S. and Srivastava, A. K., Electrical and optical response of lithium ion irradiated polyimide (kapton). *Radiat. Eff. Defects Solids*, 2001, **153**, 325–334.
32. Virk, H. S., Physical and chemical response of 70 MeV carbon ion irradiated Kapton-H polymer. *Nucl. Instrum. Meth. Phys. Res. B*, 2002, **191**, 739–743.
33. Zhu, Z., Liu, C., Sun, Y., Liu, J., Tang, Y., Jin, Y. and Du, J., Modification of polyethylene terephthalate under high-energy heavy ion irradiation. *Nucl. Instrum. Meth. Phys. Res. B*, 2002, **191**, 723–727.
34. Ram, M. K., Annapoorni, S. and Malhotra, B. D., Electrical properties of metal/Langmuir–Blodgett layer/semiconductive devices. *J. Appl. Polym. Sci.*, 1996, **60**, 407–411.
35. Pouget, J. P., Jozefowicz, M. E., Epstein, A. J., Tang, X. and MacDiarmid, A. G., X-ray structure of polyaniline. *Macromolecules*, 1991, **24**, 779–789.
36. Ziegler, J. F., SRIM-2003. *Nucl. Instrum. Meth. Phys. Res. B*, 2004, **219**, 1027–1036.
37. Alexander, L. E., *X-ray Diffraction Methods in Polymer Science*, Wiley, New York, 1969.
38. Hussain, A. M. P. and Kumar, A., Ion irradiation induced electrochemical stability enhancement of conducting polymer electrodes in supercapacitors. *Eur. Phys. J. Appl. Phys.*, 2006, **36**, 105–109.
39. Scrosati, B. (ed.), *Applications of Electroactive Polymers*, Chapman & Hall, London, 1993.
40. Hussain, A. M. P., Saikia, D., Singh, F., Avasthi, D. K. and Kumar, A., Effects of 160 MeV Ni^{12+} ion irradiation on polypyrrole conducting polymer electrode materials for all polymer redox supercapacitor. *Nucl. Instrum. Meth. Phys. Res. B*, 2005, **240**, 834–841.
41. Scherrer, P., *Gott. Nachr*, 1918, **2**, 98.
42. Singh, L. and Singh, R., Swift heavy ion induced modifications in polypropylene. *Nucl. Instrum. Meth. Phys. Res. B*, 2004, **225**, 478–482.
43. Kao, K. C. and Huang, W., *Electrical Transport in Solids: Organic Semiconductors*, Pergamon, Oxford, Great Britain, vol. 14, 1981.

ACKNOWLEDGEMENTS. We thank Inter University Accelerator Centre, New Delhi for providing beam time facility. We also thank Dr N. C. Mehra, University Science Instrumentation Centre, University of Delhi for his help in carrying out the SEM measurements.

Received 12 May 2009; revised accepted 14 October 2009

Formulation design of cyhalothrin pesticide microemulsion

Feng Zhao[1,*], Hong-ying Xia[2] and Jing-ling He[3]

[1]Jiangxi Key Laboratory of Organic Chemistry, Jiangxi Science and Technology Normal University, Nanchang 330013, China
[2]School of Chemistry Chemical Engineering, Jiangxi Science and Technology Normal University, Nanchang 330013, China
[3]Jiangxi Province Torch High Technology Development Corporation, Nanchang 330046, China

Microemulsion is regarded as the most promising pesticide formulation. However, the formulation of pesticide microemulsion is not easy and an efficient, scientific and inexpensive formulation design still remains elusive. Here, we present our formulation method based on the pseudo-ternary phase diagram and orthogonal design. In addition, the preparation of cyhalothrin microemulsion has been described and an explanation of the use of our approach is included.

Keywords: Cyhalothrin microemulsion, formula design, orthogonal design, pesticide formulations, pseudo-ternary phase diagram.

EMULSIFIABLE agricultural chemical formulations have been conveniently and widely used for a very long time[1]. However, emulsifiable solutions need large amounts of organic solvents such as toluene, dimethyl benzene, etc. which are harmful to man and his environment[2]. Hence, there is a demand for water-based, granular or control-release new pesticide formulations, which are clean and

*For correspondence. (e-mail: zhf19752003@yahoo.com.cn)

Table 1. A standard L_9 (3^4) matrix

	Factors			
	Content of pesticide in solvent	Methanol/Tween 60	Concentration of SDS solution	
Experiments	A (w/w)	B (w/w)	C (w/w)	Blank column
1	A_1 (30%)	B_1 (1 : 1)	C_1 (8%)	D_1
2	A_1 (30%)	B_2 (1 : 2)	C_2 (6%)	D_2
3	A_1 (30%)	B_3 (2 : 1)	C_3 (4%)	D_3
4	A_2 (25%)	B_1 (1 : 1)	C_2 (6%)	D_3
5	A_2 (25%)	B_2 (1 : 2)	C_3 (4%)	D_1
6	A_2 (25%)	B_3 (2 : 1)	C_1 (8%)	D_2
7	A_3 (20%)	B_1 (1 : 1)	C_3 (4%)	D_2
8	A_3 (20%)	B_2 (1 : 2)	C_1 (8%)	D_3
9	A_3 (20%)	B_3 (2 : 1)	C_2 (6%)	D_1

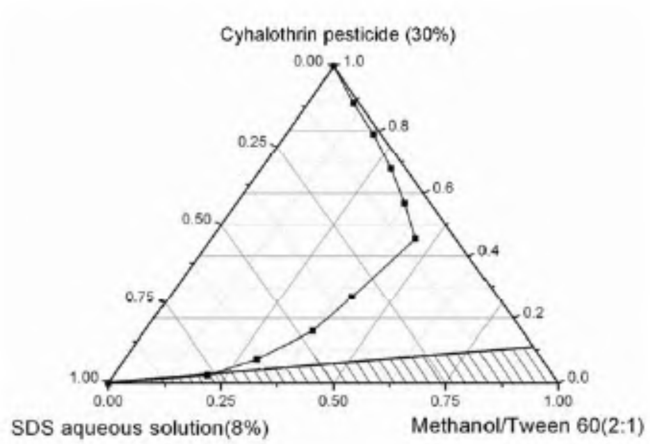

Figure 1. Pseudo-ternary phase diagram defined by $A_1B_3C_1$.

safe and have minimal impact on the environment. Amongst these, pesticide microemulsion formulation has been very popular[3].

At present, study of pesticide microemulsion is only limited to the combination of various components[3,6–8] and the trials and errors of the formulators. Very few have paid attention to the study of methodology of preparation of pesticide microemulsions[9,10].

In this paper, we report our methods based on the pseudo-ternary phase diagram and orthogonal design. Experimental results show that this method is simple and effective and can be used in the preparation of pesticide microemulsion.

The materials used for the formulation of pesticide microemulsion are: cyhalothrin pesticide sample (98%) from Jiangxi Guixi Haili Chemical Agricultural Chemicals Co Ltd. China; Tween 60 and sodium dodecyl sulfate (SDS) from Beijing Xi Zhong Chemical Factory, China; analytical reagent grade, dimethyl benzene, methanol and ethanol from Beijing Chemical Reagents Company, China and distilled water.

The pseudo-ternary phase diagram can be plotted using water titration method as described earlier[11–14]. Cyhalothrin pesticide was dissolved in dimethyl benzene as an oil phase, Tween-60 and cosurfactant methanol were mixed at certain weight ratios to obtain the surfactant mixture. Then the mixture of the oil phase and surfactant phase at weight ratios of 1 : 9, 2 : 8, 3 : 7, 4 : 6, 5 : 5, 6 : 4, 7 : 3, 8 : 2, and 9 : 1 were diluted with SDS aqueous solution at various concentrations. Phase diagrams were drawn based on visual inspection at ambient temperature.

A standard orthogonal array matrix (L9; 3^4) was constructed with three factors and three levels (Table 1) to select optimum formulation conditions to obtain a broader region of pesticide microemulsion in the phase diagrams. The characteristic value used in this experimental design was the infinite dilution area with water in the phase diagrams.

Orthogonal experiments were repeated thrice and the average results are presented in Table 2. Additionally, $\overline{K}_1$, $\overline{K}_2$, $\overline{K}_3$, averages of microemulsion existence area in the phase diagrams for three factors under different levels are listed in Table 3. The difference between the highest and the lowest among $\overline{K}_1$, $\overline{K}_2$, $\overline{K}_3$ is defined by the symbol R. Higher the R, greater the effect on the objective function.

Here, $\overline{K_{1A}}$ of factor A is calculated by

$$\overline{K_{1A}} = \frac{8.77+10.72+7.37}{3} = 8.95$$

R of factor A is calculated by

$$R = 8.95 - 7.77 = 1.18.$$

Table 3 shows that the order of the three factors' effect on the infinite dilution area with water is $R_C > R_B > R_A$.

According to R analysis from the orthogonal experiments, optimal conditions were found to be $A_1B_3C_1$ with the maximum infinite dilution area with water. To confirm the result of the orthogonal experiments, the pseudo-ternary phase diagram determined by $A_1B_3C_1$ (namely 30% content of pesticide in dimethyl benzene, methanol/

Table 2. Experimental results for a standard L_9 (3^4) matrix

	Factor					
	Content of pesticide in solvent (dimethyl benzene)	AE600/ AE500	Methanol/ (AE600+ AE500)	Blank column		
Experiment	A (w/w)	B (w/w)	C (w/w)	D	Phase diagrams	Area* M%
1	A_1 (20%)	B_1 (1 : 1)	C_1 (3 : 10)	D_1	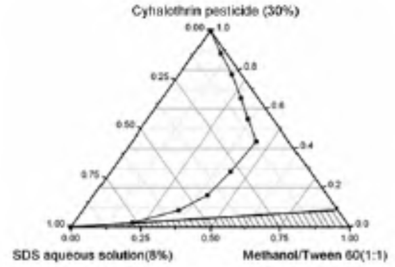	8.77
2	A_1 (20%)	B_2 (2 : 1)	C_2 (5 : 10)	D_2	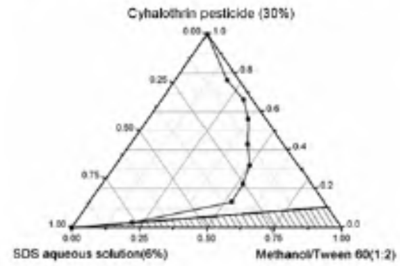	10.72
3	A_1 (20%)	B_3 (3 : 1)	C_3 (7 : 10)	D_3	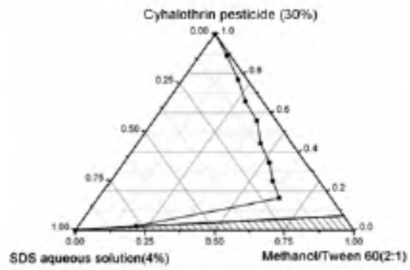	7.37
4	A_2 (30%)	B_1 (1 : 1)	C_2 (5 : 10)	D_3	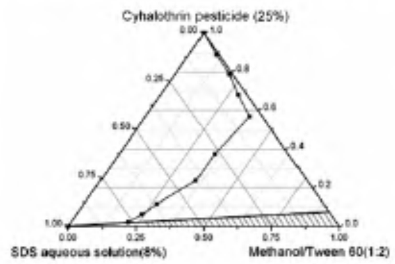	7.69
5	A_2 (30%)	B_2 (2 : 1)	C_3 (7 : 10)	D_1	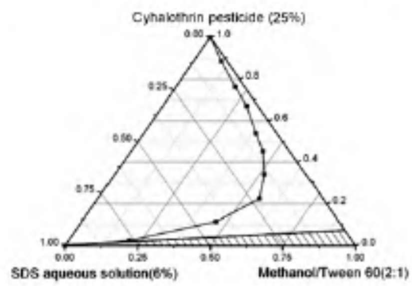	7.44

(*Contd*)

Table 2. (*Contd*)

	Factor					
	Content of pesticide in solvent (dimethyl benzene)	AE600/ AE500	Methanol/ (AE600+ AE500)	Blank column		
Experiment	A (w/w)	B (w/w)	C (w/w)	D	Phase diagrams	Area* M%
6	A_2 (30%)	B_3 (3 : 1)	C_1 (3 : 10)	D_2	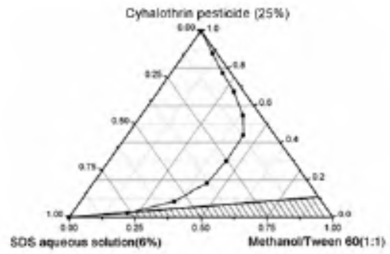	11.0
7	A_3 (40%)	B_1 (1 : 1)	C_3 (7 : 10)	D_2	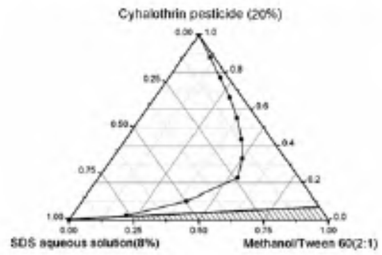	7.12
8	A_3 (40%)	B_2 (2 : 1)	C_1 (3 : 10)	D_3	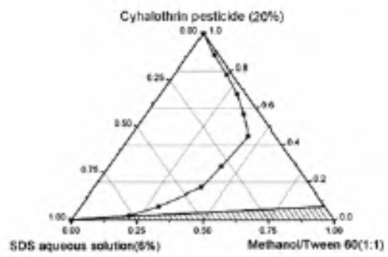	7.44
9	A_3 (40%)	B_3 (3 : 1)	C_2 (5 : 10)	D_1	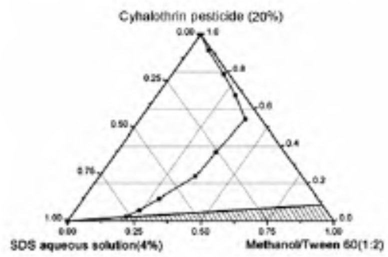	8.76

*The response value is the infinite dilution area with water.

Table 3. Analysis of experimental data

	Factor		
	A	B	C
$\overline{K}_1$	8.95	7.86	9.07
$\overline{K}_2$	8.71	8.53	9.06
$\overline{K}_3$	7.77	9.043	7.31
R	1.18	1.183	1.76

Tween 60 = 2 : 1 and SDS concentration of 8% w/w) was constructed (Figure 1).

The optimal value obtained from Figure 1 is 11.7%, and Figure 1 confirms the results from orthogonal experiments and the optimization results. The shaded region of microemulsion marked with diagonal lines in Figure 1 is the infinite dilution region, which is the best region for formation of pesticide microemulsion. So the range of pesticide microemulsion components and concentrations were obtained. However, whether the selected region is appropriate for practical applications depends on further evaluations such as heat storage stability, cold storage stability and determination of effective content and efficacy. Studies on these aspects are in progress.

Based on the pseudo-ternary phase diagram and orthogonal design, we can intuitively know the relationship between various components in a microemulsion, thus reducing the number of trials. The most potential formula of cyhalothrin microemulsion can be obtained through our approach. Experimental results show that our method is simple and effective and can be of great theoretical significance in the preparation of other pesticide microemulsions.

1. Knowles, D. A., Formulation of agrochemicals. In *Chemistry and Technology of Agrochemical Formulations* (ed. Knowles, D. A.), Springer, 1998, pp. 45–46.
2. Knowles, A., Recent developments of safer formulations of agrochemicals. *Environmentalist*, 2008, **28**, 35–44.
3. Pratap, A. P. and Bhowmick, D. N., Pesticides as microemulsion formulations. *J. Disper. Sci. Technol.*, 2008, **29**, 1325–1330.
4. Paul, B. K. and Moulik, S. P., Uses and applications of microemulsions. *Curr. Sci.*, 2001, **80**, 990–1001.
5. Prince, L. M., Emulsions and emulsion technology. In *Surfactant Science Series* (ed. Lissant, K. J.), Marcel Dekker Inc, New York, vol. 6, part I, pp. 126–127.
6. Narayanan, K. S., Water-based microemulsion formulations. United States Patent, 1994, Patent No. 5317042.
7. Narayanan, K. S., Water-based microemulsions of a triazole fungicide. United States Patent, 1994, Patent No. 5326789.
8. Jon, D. I., Prettypaul, D. I., Benning, M. J., Narayanan, K. S. and Ianniello, R. M., Water-dilutable, microemulsion concentrate and pour-on formulations thereof. United States Patent, 1999, Patent No. 5968990.
9. Skelton, P. R., Munk, B. H. and Collins, H. M., Formulation of pesticide microemulsions. In *Pesticide Formulations and Application Systems* (eds Hovde, D. A. and Beestman, G. B.), American Society for Testing and Materials, Philadelphia, 1988, pp. 36–45.
10. Hiromoto, B., Pesticide microemulsions and dispersant/penetrant formulations. United States Patent, 2007, Patent No. US 7297351.
11. Watnasirichaiku, S., Davies, N. M., Rades, T. and Tucker, I. G., Preparation of biodegradable insulin nanocapsules from biocompatible microemulsions. *Pharm. Res.*, 2000, **17**, 684–689.
12. Chen, H. B. *et al.*, A study of microemulsion systems for transdermal delivery of triptolide. *J. Control. Release*, 2004, **98**, 427–436.
13. Zhang, Q. Z., Jiang, X. G., Jiang, W. M., Lu, W., Su, L. N. and Shi, Z. Q., Preparation of nimodipine-loaded microemulsion for intranasal delivery and evaluation on the targeting efficiency to the brain. *Int. J. Pharm.*, 2004, **275**, 85–96.
14. Boonme, P., Krauel, K., Graf, A., Rades, T. and Junyaprasert, V. B., Characterization of microemulsion structures in the pseudoternary phase diagram of isopropyl palmitate/water/Brij97:1-butanol. *AAPS PharmSciTech.*, 2006, 7, E99–E104.

Received 17 May 2009; revised accepted 10 September 2009

Subtrappean Mesozoic sediments in the Narmada basin based on travel time and amplitude modelling – a revisit to old seismic data

A. R. Sridhar, A. S. S. S. R. S. Prasad, N. Satyavani and Kalachand Sain*

National Geophysical Research Institute,
(Council of Scientific and Industrial Research), Uppal Road,
Hyderabad 500 606, India

Of late, the search for hydrocarbons amidst Mesozoic sediments hidden below high-velocity Deccan Traps has gained prominence in the quest for delineating new reserves of energy. The presence of Mesozoics is directly evident in the form of a low velocity layer (LVL) prominently indicated on the refraction records. To delineate such sediments, seismic refraction/wide angle reflection studies were carried out in different parts of India. Seismic data from the Deep Seismic Sound profile in the western part of the Narmada–Son lineament (NSL) that passes through the Narmada and Tapti rivers is used for this study. Since imaging of LVL is not possible from the refraction data alone, we have used travel time skips on the refraction records along with reflections from the top and bottom of the LVL. Data from reciprocal shot points are used for confirmation and precise delineation. The analysis of seismic refraction and wide angle reflection data shows a possible existence of low-velocity Mesozoic sediments of considerable thickness sandwiched between the high velocity thick Deccan Traps and the basement.

Keywords: Deccan traps, low velocity layer, Mesozoics, Narmada–Son lineament.

DEEP seismic sounding (DSS) studies have been undertaken by National Geophysical Research Institute (NGRI) in different geological/tectonic provinces of India to explain the tectonics and unravel the evolutionary processes of various regions such as the Himalayas, Delhi–Aravalli fold belt, Central India, Cuddapah basin, Mahanadi basin, Bengal basin, Koyna region, Saurashtra and Kutch, Dharwar craton and the Southern granulite terrain, etc. All these investigations were remarkably successful and provided the key inputs for understanding the geodynamics of respective regions. The near surface geological patterns are manifestations of deep-seated structural variations and thus the shallow structure is in general, controlled by the deep crustal structure. The irregularities and the distribution of the structural patterns like faults and fractures are associated with mineral deposits[1]. The low velocity layers overlain by hard

*For correspondence. (e-mail: kalachandsain@yahoo.com)